

# Ionic coupling of hyaluronic acid with ethyl *N*-lauroyl L-arginate (LAE): Structure, properties and biocide activity of complexes

Ana Gamarra<sup>a</sup>, Beatriz Missagia<sup>b</sup>, Lourdes Urpí<sup>a</sup>,  
Jordi Morató<sup>b</sup>, Sebastián Muñoz-Guerra<sup>a\*</sup>

<sup>a</sup>*Departament d'Enginyeria Química, Universitat Politècnica de Catalunya,  
ETSEIB, Diagonal 647, Barcelona 08028, Spain.*

<sup>b</sup>*Health and Environmental Microbiology Lab & UNESCO Chair on Sustainability, Universitat Politècnica  
de Catalunya, ESEIAAT, Edifici Gaia, Pg. Ernest Lluch/Rambla Sant Nebridi, Terrassa 08222, Spain*

E-mail: [sebastian.munoz@upc.edu](mailto:sebastian.munoz@upc.edu)

## 1 **Abstract**

2 Ethyl <sup>α</sup>*N*-lauroyl L-arginate hydrochloride (LAE) was coupled with hyaluronic acid (HyA)  
3 to form ionic complexes with LAE to HyA ratios of 1:1 and 1:2. The complexes were extensively  
4 characterized by FTIR and NMR spectroscopies and their thermal properties evaluated by  
5 thermogravimetry and calorimetry. Thin films prepared from these complexes by casting  
6 displayed a smectic-like structure based on an ordered arrangement of LAE and HyA layers  
7 with a nanometric periodicity of 3.8-3.9 nm. Films immersed in water at pH 7.4 and 5.5  
8 dissociated to deliver free LAE to the environment and reaching the equilibrium in few hours.  
9 The biocide activity of these films against both Gram-positive and Gram-negative bacteria was  
10 preliminary assessed by the liquid medium method, and shown to be notable in both cases. The  
11 antibacterial property of the complexes was found to increase with the content of LAE and to be  
12 particularly efficient against Gram-negative *S. enterica* bacteria.

## 13 1. Introduction

14       Complexation of polyelectrolytes with counter-ions of low molecular weight is a relatively  
15 simple approach recurrently used for creating materials that largely differ in properties from the  
16 parent polymer. This is so because coupling between complementary ionic building-blocks  
17 usually leads to molecular arrangements able to self-assemble in well-organized nanostructures  
18 ([Macknight, Ponomarenko, & Tirrell, 1998a](#)). The complexes made of ionic polypeptides and  
19 tetraalkylsurfactants constitute a representative example of these systems ([Hanski et al., 2006](#);  
20 [Macknight, Ponomarenko, & Tirrel, 1998b](#); [Pérez-Camero et al., 2004](#); [Ponomarenko, Waddon,](#)  
21 [Tirrell, & MacKnight, 1996](#)). These complexes tend to adopt a layered biphasic structure with  
22 crystallinity depending on the length of the surfactant alkyl chain and a periodical spacing  
23 sensitive to temperature. Negatively charged polysaccharides, and in particular polyuronic  
24 acids, have been demonstrated to behave in a way not far from that described for anionic  
25 polypeptides. Thus coupling of alginic, pectinic and hyaluronic acids with  
26 alkyltrimethylammonium surfactants has been recently reported to render stable ionic  
27 complexes arranged in layers showing order at the nanometric scale ([Tolentino, Alla, Martínez](#)  
28 [de Ilarduya, & Muñoz-Guerra, 2011, 2013](#)).

29       In this paper we wish to report on ionic complexes made from hyaluronic acid and an  
30 arginine-based compound, namely ethyl  $\alpha$ -N-lauroyl L-arginate hydrochloride (LAE), which are  
31 able to display antimicrobial properties. Due to the increasing resistance of bacteria to  
32 antibiotics, bactericide polymers start to be considered today as an attractive antiseptic  
33 alternative ([Engler et al., 2012](#)). In such systems, the polymer acts as a matrix for holding and  
34 controlling the release of the antimicrobial agent so that the possible toxicity associated to the  
35 biocide is largely repressed and the period of activity increased when compared to the neat  
36 biocide. During the last decade the attention given to polymeric materials with antimicrobial  
37 activity has been very noticeable ([Santos et al., 2016](#)) and some hyaluronic acid-based  
38 materials incorporating antimicrobial agents may be found in the recent literature. HyA-silver

39 nanoparticles and HyA coupled with polyhexanide (Baier et al, 2013; Kemp et al., 2009), and  
40 nisin polypeptide (Lequeux, Ducasse, Jouenne, & Thebault, 2014) are representative examples  
41 of such materials. To our knowledge, no study addressed to examine the ionic LAE·HyA  
42 complexes including their antimicrobial activity has been described so far.

43 Hyaluronic acid (HyA) is a high molecular weight mucopolysaccharide composed of  
44 repeating disaccharide units of  $\beta$ -1,3-*N*-acetyl D-glucosamine and  $\beta$ -1,4-D-glucuronic acid with a  
45 great capacity to retain moisture and to form hydrogels with excellent viscoelastic properties.  
46 Furthermore HyA is high biocompatible, non-immunogenic and susceptible to biodegradation by  
47 human hyaluronidases. HyA is always present in the human body in small amounts, and it is  
48 widely used in medicine, cosmetic and veterinary surgery (Necas, Bartosikova, Brauner, &  
49 Kolar, 2008; Stern, Kogan, Jedrzejewski, & Šoltés, 2007). The polysaccharide may be chemically  
50 modified to render biomaterials with properties suitable for tissue engineering (Allison & Grande-  
51 Allen, 2006; Burdick & Prestwich, 2011; Schanté, Zuber, Herlin, & Vandamme, 2011). Rooster  
52 combs were the traditional source of HyA but today it is mainly produced by microbial  
53 fermentation which has boosted its applications and raised its commercial value (Liu, Liu, Li, Du,  
54 & Chen, 2011). On the other hand, LAE is a synthetic surfactant consisting of an ethyl esterified  
55 arginine head with a lauroyl tail attached to the  $\alpha$ -amino group. LAE is widely recognized as a  
56 highly powerful preservative agent for a large variety of food-borne bacteria (Becerril, Manso,  
57 Nerin, & Gómez-Lus, 2013; Otero et al., 2014) a property that is due to its ability for altering the  
58 microorganisms metabolism without producing cellular disruptions (Rodriguez, Seguer,  
59 Rocabayera, & Manresa, 2004). LAE has been assessed to be nontoxic and it has been  
60 classified by FDA (Food and Drug Administration) as GRAS (Generally Recognized as Safe) at  
61 concentrations up to 200 ppm. According to their biological properties, ionic coupling of LAE  
62 with HyA is envisaged as a very convenient approach to build antimicrobial films with potential  
63 use in food preservation and design of medical antiseptic devices.

64 The working hypothesis for this research is that LAE-HyA complexes will be readily  
65 formed with prefixed compositions, and that they will show strong activity against pathogens  
66 because LAE will be released under control to the wet environment by water-mediated  
67 dissociation of the ionic pair. LAE and HyA are largely expected to combine ionically because  
68 both compounds have been reported to form stable ionic complexes when they enter in contact  
69 with diverse counter-ions. Thus LAE is known to interact positively with the anionic  
70 polysaccharides present in the food (Asker, Weiss, & McClements, 2009; Loeffler et al., 2014),  
71 and complexes of HyA with a diversity of organocationic compounds have been also described  
72 (Battistini et al., 2017; Bračič, Hansson, Pérez, Zemljič, & Kogej, 2015; Chytil, Trojan, &  
73 Kovalenko, 2016; Tolentino, Alla, Martínez de Ilarduya, & Muñoz-Guerra, 2013). Complexes of  
74 LAE with poly( $\gamma$ -glutamic acid) (LAE-PGGA) with antibacterial properties have been recently  
75 described by us (Gamarra-Montes, Missagia, Morató, & Muñoz-Guerra, 2017).

76 In this paper cationic LAE is coupled with the polyanionic hyaluronic acid to obtain the  
77 ionic complexes abbreviated as LAE-HyA with LAE to HyA ratios of either 1:1 or 1:2. These  
78 complexes are extensively characterized by different techniques (FT-IR, NMR, TGA, DSC, XRD  
79 and POM) and paying detailed attention to the nanostructure. Then the release rate of LAE from  
80 complexes is estimated under different conditions and the antimicrobial properties of the films  
81 are evaluated in vitro experiments against both Gram-positive (*L. monocytogenes* and *S.*  
82 *aureus*) and Gram-negative bacteria (*S. enterica* and *E.coli*).

## 83 **2. Experimental**

### 84 *2.1. Materials*

85 The sample of sodium salt of hyaluronic acid (Na-HyA) with a weight-average of 50,000  
86 Da was purchased from Enze Chemicals. The  $^1\text{H}$  NMR spectrum ascertaining the identity of this  
87 sample is provided in the Supplementary Material file (SM) associated to this article (Figure S1).

88 The sample of Ethyl  $\alpha$ -N-lauroyl L-arginate hydrochloride (LAE) used in this work was a kind gift  
89 from Vedeqsa Grupo LAMIRSA (Terrassa, Barcelona).

## 90 2.2. *Measurements*

91 FTIR spectra within the 4000-600 nm range were recorded from powder samples on a  
92 Perkin Elmer Frontier equipment provided with an ATR accessory.  $^1\text{H}$  NMR spectra were  
93 recorded on a Bruker AMX-300 NMR instrument operating at 300.1 MHz. Samples were  
94 dissolved in deuterated methanol and TMS was used as internal reference. Thermogravimetric  
95 analysis (TGA) was performed over the 30 to 600  $^{\circ}\text{C}$  interval at a heating rate of  $10\text{ }^{\circ}\text{C}\cdot\text{min}^{-1}$   
96 under an inert atmosphere on a Mettler-Toledo TGA/DSC 1 Star System thermobalance.  
97 Sample weights of 10-15 mg were used for this analysis. Differential scanning calorimetry  
98 (DSC) was carried out on a Perkin-Elmer DSC 8000 instrument calibrated with indium and zinc.  
99 Heating-cooling cycles at a rate of  $10\text{ }^{\circ}\text{C}\cdot\text{min}^{-1}$  under a nitrogen atmosphere within the -30 to  
100 200  $^{\circ}\text{C}$  temperature range were applied for the analysis using sample weights of 2-5 mg. X-ray  
101 diffraction studies were performed using X-ray synchrotron radiation at the BL11 beamline  
102 (NCD, Non-Crystalline Diffraction) of ALBA synchrotron in Cerdanyola del Vallès, Barcelona.  
103 Simultaneous SAXS and WAXS were taken in real time from powder samples subjected to  
104 heating-cooling cycles at a rate of  $10\text{ }^{\circ}\text{C}\cdot\text{min}^{-1}$ . The radiation energy employed corresponded to  
105 0.1 nm wavelength, and spectra were calibrated with silver behenate ( $\text{AgBh}$ ) and  $\text{Cr}_2\text{O}_3$  for small  
106 and wide angle diffraction, respectively. Optical microscopy was carried out on an Olympus  
107 BX51 polarizing optical microscope (POM) equipped with a digital camera and a Linkam THMS-  
108 600 hot stage provided with nitrogen gas circulating system. Samples for POM observation  
109 were prepared by evaporation at room temperature of a 3 % (w/w) solution of the complex in  
110 methanol placed between microscope cover slides.

### 111 2.3. Complexes formation and film preparation

112 The methodology used by (Ponomarenko, Waddon, Tirrell, & MacKnight, et al.,1996) for  
113 the preparation of ionic complexes from poly( $\alpha$ -amino acids) and ionic surfactants was applied  
114 in this work. This methodology with some slight modifications has been used by us for the  
115 synthesis of complexes made from either PGGA or polyuronic acids and quaternary  
116 tetraalkylammonium salts bearing long linear alkyl chains containing from 12 to 22 carbon  
117 atoms (Pérez-Camero et al., 2004; Tolentino, Alla, Martínez de Ilarduya, & Muñoz-Guerra,  
118 2011a, 2013) and also for the preparation of LAE-PGGA complexes (Gamarra-Montes,  
119 Missagia, Morató, & Muñoz-Guerra, 2017). The procedure applied here is essentially as follows:  
120 A solution of LAE hydrochloride in water was slowly poured into a solution of NaHyA in water  
121 under mild stirring at a temperature around 35 °C. The complex precipitated as a white powder  
122 after several hours of standing. The precipitate was recovered by centrifugation and repeatedly  
123 washed with water and finally dried under vacuum for at least 48 h. Complexes were prepared  
124 from mixtures containing both 1:1 and 1:2 molar ratios of LAE to HyA, and they are abbreviated  
125 as LAE-HyA-1 and LAE-HyA-0.5, respectively.

126 Consistent films made of LAE-HyA complexes were prepared by casting a solution of the  
127 complex in methanol on 3x3 cm<sup>2</sup> Petri plates and leaving it to dry at room temperature for 24 h.  
128 Films were cut in 1x1 cm<sup>2</sup> squares and further dried under vacuum for 24 h. Film thickness were  
129 estimated to be 105 ± 5 µm as measured by using a Mitutoyo micrometer (Osaka, Japan).

### 130 2.4. Complex dissociation and bactericide activity

131 For evaluation of the dissociation of LAE-HyA complexes upon incubation in aqueous  
132 medium, LAE-HyA complex films were suspended in 2 mL of buffer and the suspension placed  
133 into cellulose membrane tubes (2000 Da cut-off) and dialysis performed against 10 mL of the  
134 same buffer for a week. Assays were carried out at pH= 7.4 and 5.5 at 25 °C, and the amount of  
135 LAE released to the environment was determined by measuring the absorbance of the dialysate

136 at 220 nm at prefixed incubation times. Aqueous buffers used for incubation were prepared from  
137 mixtures of disodium hydrogen phosphate and potassium hydrogen phosphate according to the  
138 European Pharmacopea 5.0.

139 The antimicrobial activity of LAE-HyA complexes over time was tested in vivo against both  
140 Gram-negative and Gram-positive bacteria in liquid culture media. Cultures of *S. enterica* CECT  
141 4594, *E. coli* NCTC 9001, *L. monocytogenes* ATCC 19115 and *S. aureus* ATCC 6538 were  
142 obtained from the National Collection of Type Cultures (NCTC, Public Health England, UK), the  
143 Spanish Type Culture Collection (CECT, Valencia, Spain) and the American Type Culture  
144 Collection (ATCC, USA), respectively. The organisms were stored at -20°C in tryptic soy broth  
145 (TSB; Merck, Darmstadt, Germany) containing 50% (v/v) glycerol until used. To activate them, a  
146 loopful of each bacterium was spread to give single colonies on tryptic soy agar (TSA; Difco  
147 Laboratories) petri dishes, and incubated at 37 °C for 24 h. Representative colonies were then  
148 picked out and suspended into 10 mL tubes of TSB pH 7.0, and incubated at 37 °C for 24 hours  
149 to obtain early stationary phase cells (optical density of 0.9 at 600 nm). The cultures were then  
150 inoculated (100 µL) into fresh TSB, and incubated at 37 °C for 18 h to reach the exponential  
151 phase (optical density of 0.2 at 600 nm). At this stage the bacteria cultures were diluted to  
152 obtain a concentration of 10<sup>5</sup> CFU·mL<sup>-1</sup>. 100 µL of these bacterial suspensions were then  
153 transferred to sterile tubes containing an approximate 1 cm<sup>2</sup>-film piece of HyA (negative control),  
154 LAE-HyA-1, or LAE-HyA-0.5 in 10 mL of fresh TSB. The tubes were placed in a thermostated  
155 oven at 37 °C and 100 µL aliquots were removed from the suspension at selected periods of  
156 time (2, 8 and 24 hours), diluted with peptone water (1% v/v), and plated in petri dishes with 15  
157 mL of TSA culture medium. A bacterial suspension prepared in the same way but without film  
158 added was used as blank. Quantification of colonies was made in triplicates and data are  
159 represented as logarithm of colony forming units (Log(CFU)). Formulae used for logarithm  
160 reduction value (LRV) and percent reduction calculation were the following (Durán, Marcato, De  
161 Souza, Alves, & Esposito, 2007),

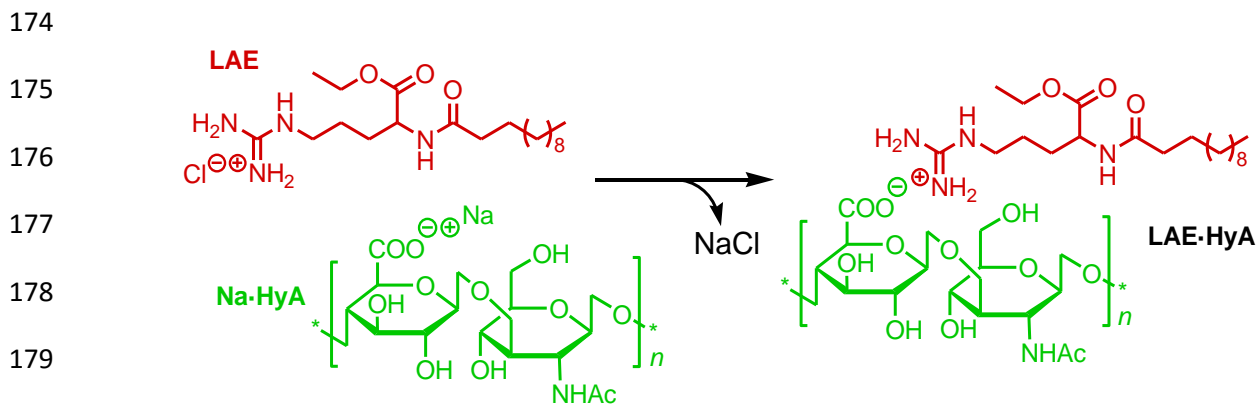
162 Log reduction value =  $\log_{10}(A/B)$  Percentage reduction =  $[(A-B)/A] \cdot 100$

163 where A and B are the number of viable bacteria in the negative control and after treatment with  
164 either LAE·HyA-1 or LAE·HyA-0.5.

### 165 3. Results and discussion

#### 166 3.1. Synthesis of complexes

167 The preparation of LAE·HyA complexes was performed according to Scheme 1. Mixing at  
168 35 °C of the two aqueous solutions containing LAE and Na·HyA, respectively, rendered the  
169 complex as a white precipitated that could easily recovered by centrifugation. Two LAE·HyA  
170 molar ratios, *i.e* 1:1 and 1:2, were used at mixing with the purpose of obtaining complexes with  
171 equal or half molar amount of LAE respect to HyA. The <sup>1</sup>H NMR analysis revealed that the  
172 actual compositions of the complexes were very close to those used for feeding with a slight  
173 deficiency in the cationic component. Data related with the synthesis are given in Table 1.



182 **Scheme 1.** Formation of LAE·HyA complexes by coupling reaction of LAE with hyaluronic acid. LAE to  
183 HyA ratios of 1:1 and 1:2 were used.

#### 183 3.2. Chemical characterization

184 The FTIR spectra recorded from the LAE·HyA complexes are shown in Figure 1 together  
185 with those of Na·HyA and LAE and their interpretation was supported by previously reported



186 data of the two components (Gilli et al., 1994; Gamarra, Missagia, Morató, Muñoz-Guerra,  
 187 2017). The spectra of the complexes include the bands characteristic of the two counterparts  
 188 with relative intensities according to composition. In fact, the digital region of these spectra over  
 189 the 1800-650  $\text{cm}^{-1}$  may be made to correspond to the overlapping of those observed for HyA  
 190 and LAE with their contributions being proportional to their contents in the complexes. In  
 191 particular the bands characteristic of LAE appearing at 1526 and 1176  $\text{cm}^{-1}$  are detected in the  
 192 complexes with intensity increasing with the LAE:HyA ratio. Also the bands at 2917 and 2840  
 193  $\text{cm}^{-1}$  due to the stretching of C-H bonds, which are shared by the two components but with much  
 194 higher intensity in LAE, increase in parallel to the content of this compound in the complex. On  
 195 the other hand, the strong band displayed by HyA at c.a. 1030  $\text{cm}^{-1}$  and arising from C-O-C  
 196 stretching keeps the same features in the spectra of the complexes. Finally just to notice that  
 197 the broad absorption displayed by HyA in the 3500-3200  $\text{cm}^{-1}$  region, which is attributed to  
 198 hydroxyl groups, is fully retained in the complexes impeding the visualization of the weak NH  
 199 stretching peaks expected to arise from the LAE counterpart.

**Table 1.** Synthesis, thermal properties and structural data.

Compound	Synthesis results				Thermal properties				X-ray diffraction data (nm)					
					TGA <sup>d</sup>			DSC <sup>e</sup>	SAXS <sup>f</sup>			WAXS <sup>f</sup>		
	$c^a$ (M) <sup>a</sup>	$T$ (°C) <sup>b</sup>	Yield (%)	LAE:HyA <sup>c</sup>	$^oT_d$ (°C)	$^{\max}T_d$ (°C)	$W$ (%)	$T_m$ (°C)	$L_o^{10^\circ\text{C}}$	$L_o^{120^\circ\text{C}}$	$L_o^{10^\circ\text{C}}$	$d^{10^\circ\text{C}}$	$d^{120^\circ\text{C}}$	$d^{10^\circ\text{C}}$
HyA	-	-	-	-	200	228	35	-	n.d.	n.d.	n.d.	n.d.	n.d.	n.d.
LAE·HyA-0.5	0.02	35	70	0.4 :1.0	217	228/328	19	-	3.8	3.8	3.7	0.45	0.45	0.45
LAE·HyA-1	0.01	35	80	0.9 :1.0	228	259/328	11	-	3.9	3.9	3.8	0.45	0.45	0.45
LAE	-	-	-	-	245	275/311	10	62	3.0	-	-	m <sup>g</sup>	-	-

<sup>a</sup> Concentration of the two solutions mixed to form the complex.

<sup>b</sup> Mixing temperature selected according to the LAE solubility in water.

<sup>c</sup> Molar ratio of LAE to HyA in the complex estimated by <sup>1</sup>H NMR.

<sup>d</sup>  $^oT_d$  and  $^{\max}T_d$ : onset (5% weight loss) and maximum rate decomposition temperatures;  $W$ : remaining weight after heating at 600 °C.

<sup>e</sup>  $T_m$  is the melting temperature recorded by scanning calorimetry.

<sup>f</sup> Small angle (SAXS) and wide angle (WAXS) X-rays scattering recorded at 10 °C, 120 °C and 10 °C (after cooling) as indicated.

n.d.: not determined.

<sup>g</sup> Many peaks observed.

200

201

202  
203  
204  
205  
206  
207  
208  
209  
210  
211  
212  
213  
214  
215  
216  
217  
218  
219  
220  
221  
222  
223  
224  
225  
226  
227  
228  
229  
230

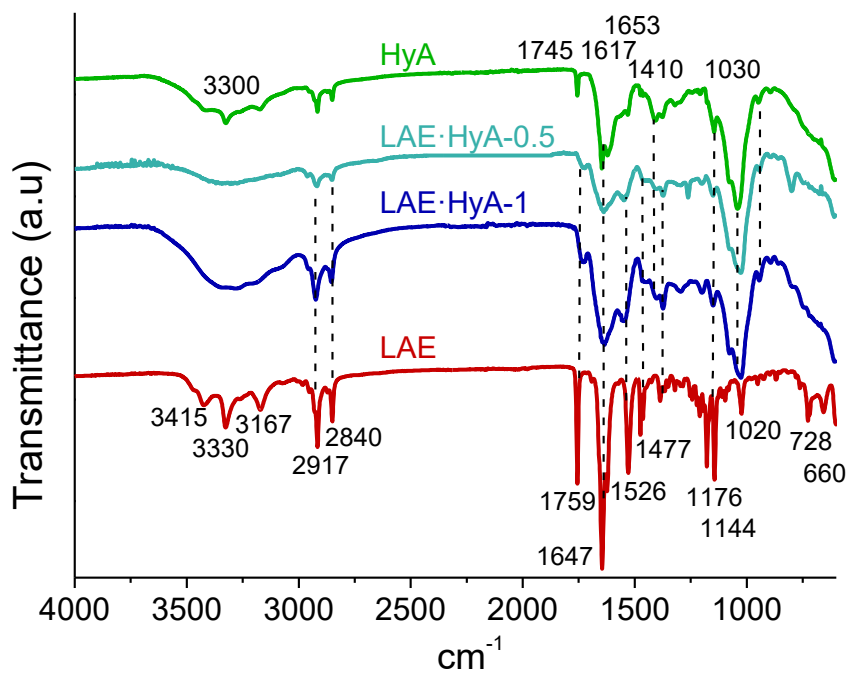
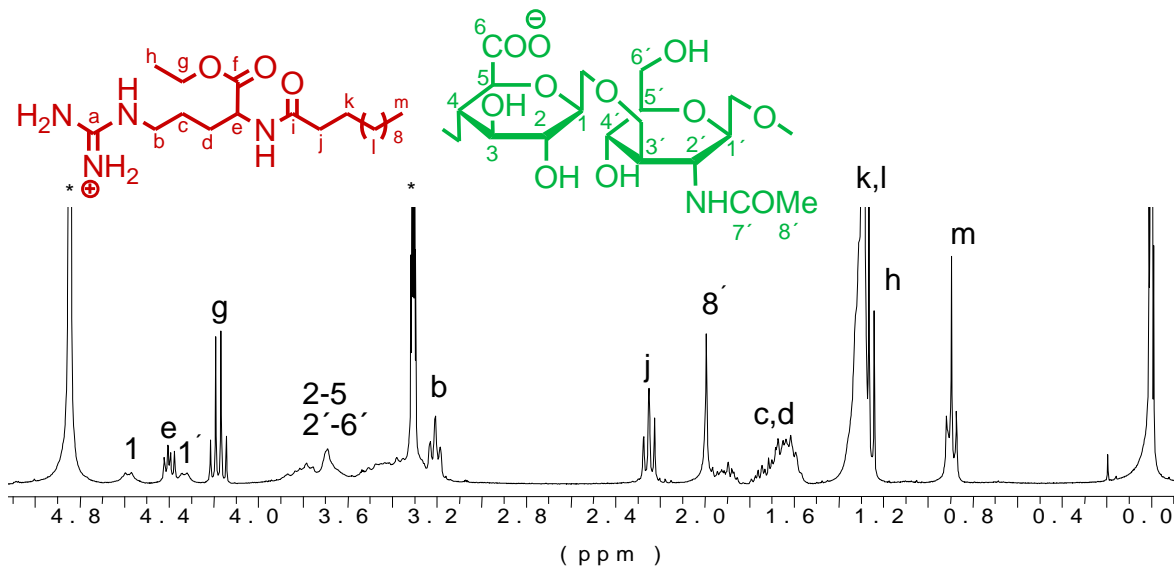


**Figure 1.** Comparison of FTIR spectra of LAE, HyA and their complexes with indication of most characteristic bands.

The <sup>1</sup>H NMR spectrum recorded from LAE-HyA-1 in methanol solution is reproduced in Figure 2 with all signals consistently assigned to the chemical structure of the complex. The spectra of LAE, HyA, and the LAE-HyA-0.5 complex may be inspected in the SM file (Figures S1 and S2). In the complexes' spectra, signals due to of the HyA counterpart are according to that reported for the complexes made from HyA and alkyltrimethylammonium surfactants (Tolentino, Alla, Martínez de Ilarduya & Muñoz-Guerra, 2013), and those arising from the surfactant counterpart coincide almost exactly with those observed in the spectrum of pristine LAE. In general signals appear well resolved although those arising from the inner methylenes of the dodecyl group of LAE appear overlapped (k,l), and those due to the protons of the pyranose rings are grouped in two undifferentiated broad signals (2-5 and 2'-6').



231 **Figure 2.**  $^1\text{H}$  NMR spectrum of LAE-HyA-1 recorded in MeOD. \*Signals arising from the solvent.

232

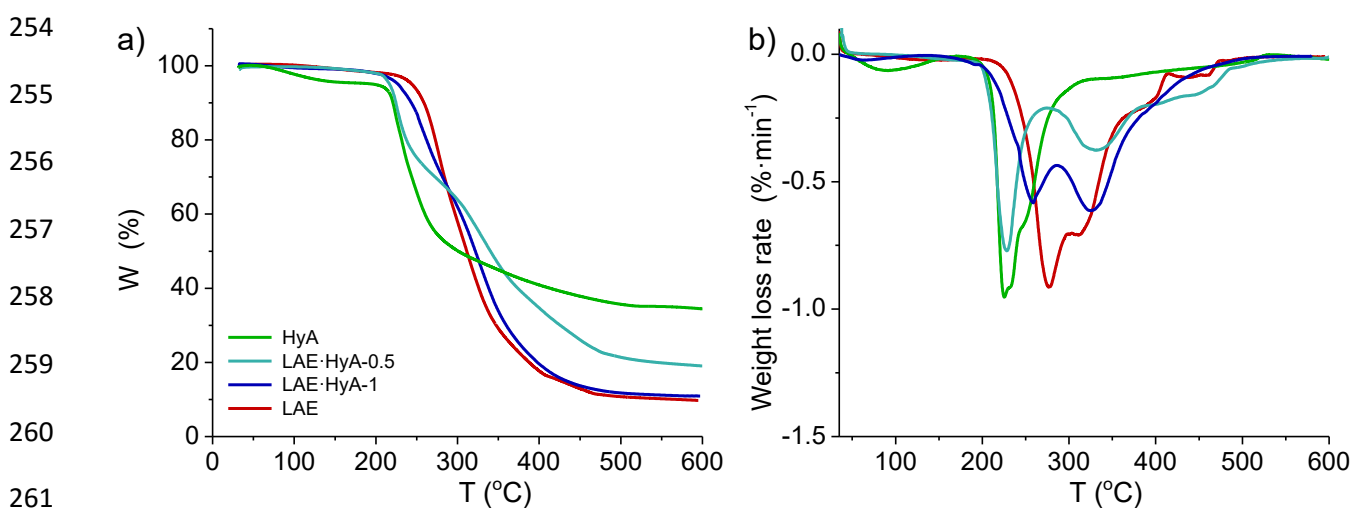
233        Signals arising from the anomeric proton of the glucuronic unit of HyA and the  $\alpha$ -  
 234 methylene protons of the lauroyl moiety of LAE (signals 1 and j) were used to determine the  
 235 composition of the complexes. The relative area quantification of these signals revealed that the  
 236 complexes have compositions very close to those used for their synthesis (Table 1), with  
 237 deviations within the range that could be expected according to results obtained for other ionic  
 238 complexes of HyA previously studied by us (Tolentino, Alla, Martínez de Ilarduya & Muñoz-  
 239 Guerra, 2013; Gamarra, Missagia, Morató, Muñoz-Guerra, 2017).

240

### 241 3.2. Thermal properties and structure

242        Firstly the thermal stability of the complexes was evaluated by TGA. The traces registered  
 243 for both LAE-HyA-1 and LAE-HyA-0.5 over the 20-600  $^{\circ}\text{C}$  were compared with those of HyA  
 244 and LAE in Figure 3a, and their respective derivative curves are represented in Figure 3b. It  
 245 should be noted that the trace of HyA shows a weight loss of about 5% at temperatures around  
 246 100  $^{\circ}\text{C}$ , which is interpreted as due to the release of the remaining adsorbed water that could  
 247 not be removed by the drying treatment applied to the sample. Nevertheless, all compounds

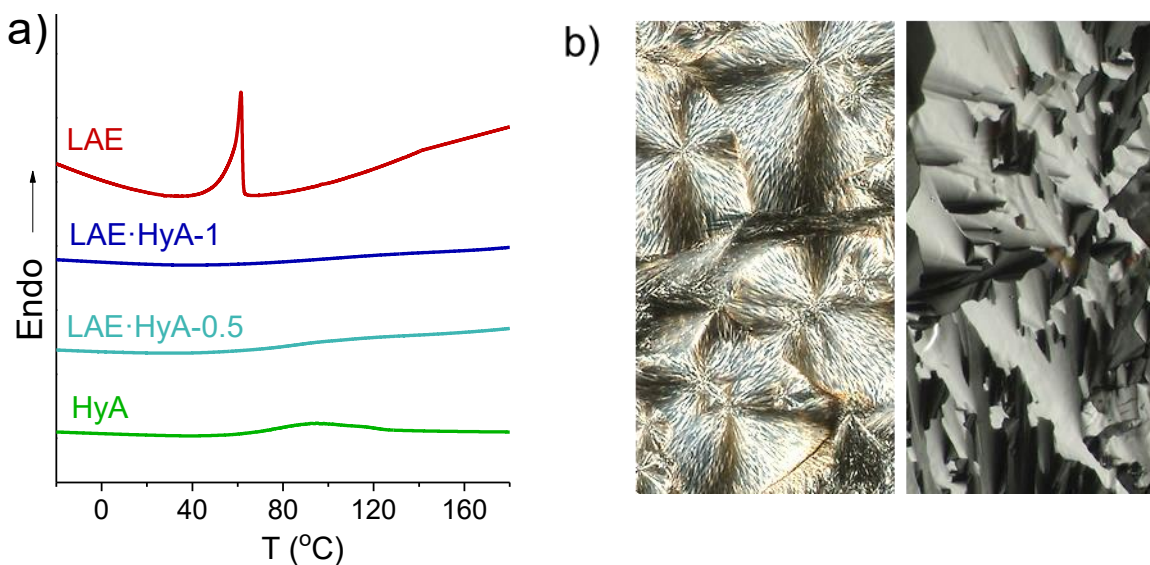
248 started to decompose above 200 °C at an onset temperature that increases with the content in  
249 LAE. Furthermore, the maximum decomposition rate in LAE took place around 50 °C higher  
250 than for HyA. These differences are reflected in the complexes which show  $^{max}T_d$  of 230 °C and  
251 260 °C for LAE-HyA-0.5 and LAE-HyA-1, respectively. It can be stated on the basis of these  
252 results that the LAE-HyA complexes could be comfortably handled in the case that usual  
253 heating processes were applied for film manufacture.



262 **Figure 3.** TGA traces of HyA, LAE and the LAE-HyA complexes recorded under an inert atmosphere (a),  
263 and their respective derivative curves (b).

264 The DSC analysis (Figure 4a) revealed that only LAE shows melting transition whereas  
265 almost plain traces were registered for HyA and their complexes (the slight endotherm  
266 appreciated on the trace of HyA in the 80-120 °C interval is very likely due to water  
267 evaporation). The crystalline nature of LAE was clearly evidenced in the spherulitic texture that  
268 is seen in films of this compound prepared by casting when they are observed by POM (Figure  
269 4b left). Accordingly, it can be concluded that the crystallinity of LAE is lost when this compound  
270 is attached to HyA. However, POM of the LAE-HyA-1 film showed a fan-like texture typical of a  
271 smectic mesophase (Figure 4b right) indicating that complexes are ordered in a crystal liquid

272 structure. A similar appearance was observed for the LAE·HyA-1 complex (Figure S3 in SM  
273 file).

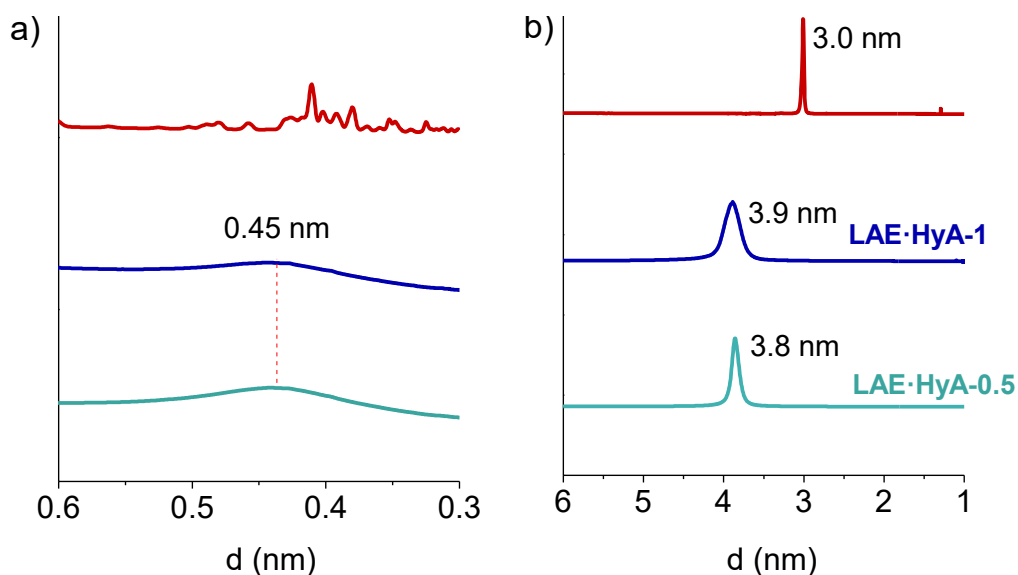


274 **Figure 4.** a) First heating DSC traces recorded from LAE and its ionic complexes. b) POM micrographs  
275 taken from LAE (left) and LAE·HyA-1 (right) thin films at 25 °C.

276 The XRD scattering recorded in the WAXS region for LAE and the complexes (Figure 5a)  
277 was in full agreement with DSC results. The trace recorded for LAE contains a large number of  
278 well-defined peaks, as it should be expected for a crystalline organic compound, whereas a  
279 broad hill centered around 0.45 nm is the only alteration appearing on the traces of the  
280 complexes. In the SAXS region (Figure 5b), spectra of both LAE and complexes show an  
281 apparent sharp peak corresponding to a repeat distance of 3.0 nm for the former and around  
282 3.9-3.8 nm for the latter. These results confirm the occurrence of an ordered arrangement at the  
283 nanometric level in the complexes in spite that they are not crystallized.

284 With the purpose of assessing the influence of temperature on these structures, samples  
285 of LAE and LAE·HyA-1 were subjected to a heating-cooling cycle over the 10-120 °C range at a  
286 rate of 10 °C·min<sup>-1</sup>, and the changes taking place in the X-ray scattering were registered over

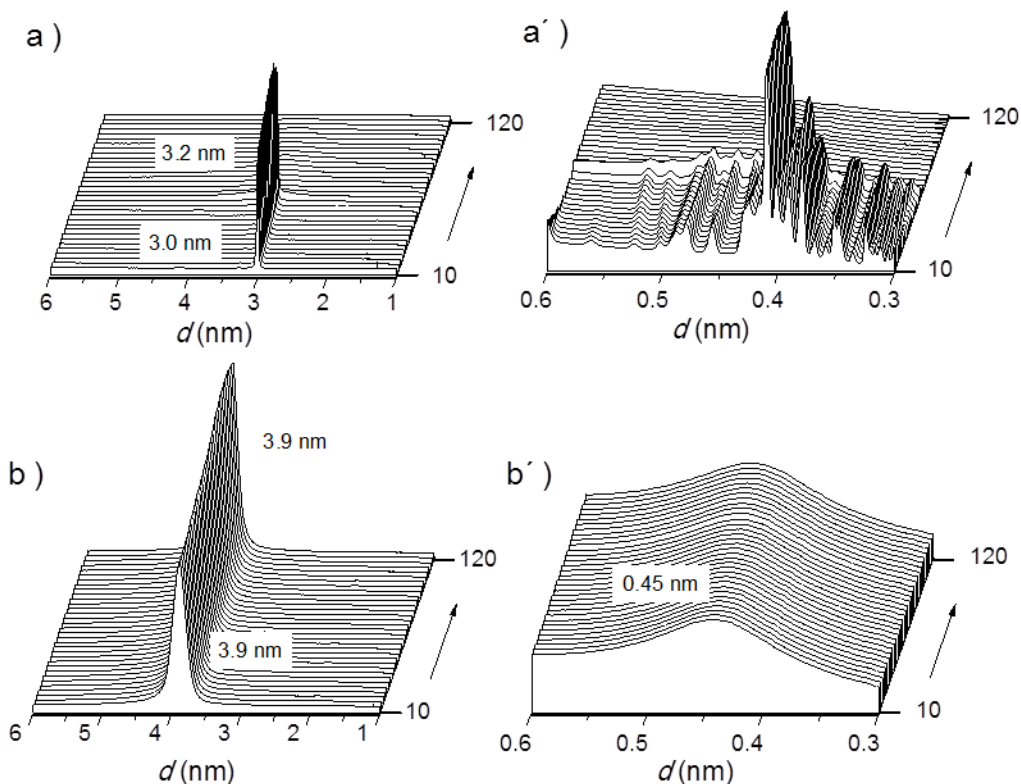
287 the whole temperature range at real time (Figure 6). Both SAXS and WAXS signals observed  
288 for LAE fully disappeared when temperature reached 60-65 °C, which is clear evidence that the  
289 structure melted and all the order initially present in the sample vanished. The cooling trace did



290 **Figure 5.** XRD profiles recorded at 10 °C from LAE and their complexes LAE·HyA in the WAXS (a) and  
291 SAXS regions (b).

not show any discrete scattering (see Figure S4 in the SM file) indicating that the initial structure present in LAE was not recovered. The behavior observed for LAE·HyA-1 was noticeably different. The 3.9 nm peak remained unchanged along the whole heating treatment bringing into evidence the stability of the mesophase up to temperatures close to 200 °C. This is consistent with the observations made by POM in which the birefringence displayed by the films of LAE·HyA-1 did not vanished when subjected to heating at similar temperatures. Similar results were obtained in the XRD/POM analysis of LAE·HyA-0.5 complex (Figures S5 in SM). It seems reasonable to assume therefore that higher temperatures are needed to destroy the liquid crystal phase adopted by these complexes, an assumption that unfortunately cannot be tested since their thermal decomposition starts to be noticeable at 215-230 °C. As much expected, the

WAXS profiles arising from the average interatomic distances present in the disordered phase made of lauroyl chains of the LAE moiety remained unperturbed along the heating treatment.

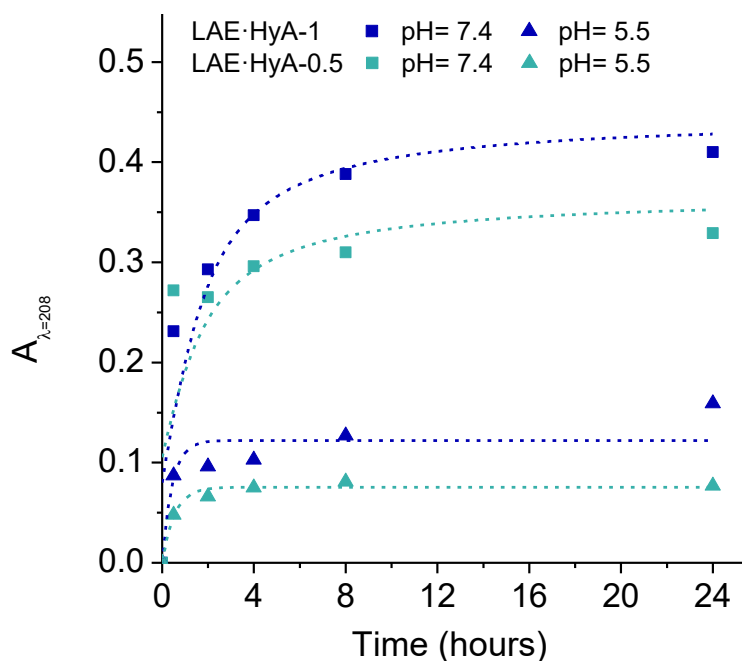


292 **Figure 6.** Evolution of the SAXS and WAXS profiles of LAE (a and a') and LAE·HyA-1 (b and b') at  
 293 heating from 10 to 120 °C.

### 294 3.3. LAE release and antimicrobial properties

295 According to the hypothesis formulated for this work, the biocide activity expected for the  
 296 LAE·HyA complexes should arise from the free LAE that is released to the environment as a  
 297 consequence of the dissociation undergone by the ionic pair upon incubation in an aqueous  
 298 medium. To evaluate the capacity of these complexes to deliver LAE under conditions  
 299 commonly found in food environments, the amount of LAE that is released from both LAE·HyA-  
 300 1 and LAE·HyA-0.5 and accumulated in the incubation medium at pH 7.4 and 5.5 was

301 measured by UV absorption at 220 nm, and results are compared in Figure 7. In all cases, the  
302 dissociation equilibrium was reached within an incubation period of 4 to 8 h. The concentration  
303 of LAE attained at that time was much higher at pH 7.4 than at pH 5.5 and, as largely expected,  
304 the accumulated amount of free LAE noticeably increased with the LAE:HyA ratio in the  
305 complex. An additional experiment carried out at pH 7.4 but at a temperature of 4 °C revealed  
306 that cooling delayed the release of LAE in an extent similar to that observed for decreasing the  
307 pH down to 5.5 (Figure S6 in SM).



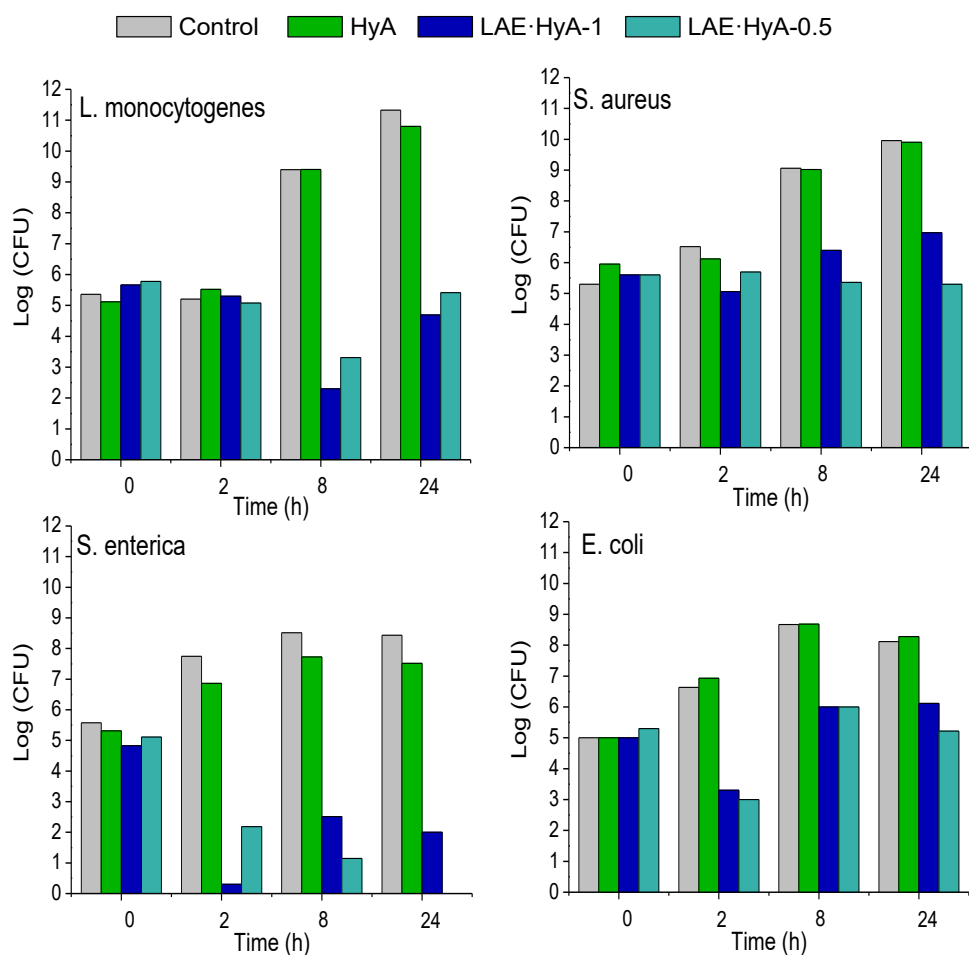
308 **Figure 7.** Dissociation of LAE·HyA complexes upon incubation in aqueous medium at pH= 7.4 and 5.5 at  
309 25 °C.

310 The bactericide activity of films made of LAE·HyA-1 and LAE·HyA-0.5 complexes at pH  
311 7.4 and 37 °C was evaluated by in vitro assays applying the liquid medium method and using as  
312 substrates two pairs of bacteria representatives of the Gram-positive (*L. monocytogenes* and *S.*  
313 *aureus*) and Gram-negative (*S. enterica* and *E. coli*) groups. A fast appraisal of the bactericidal  
314 effect could be made by visual inspection of the tubes which revealed disappearance of the



315 initial turbidity for all the cases after 24 h of incubation (Figure S7, SM file). Quantitative results  
316 of these preliminary assays expressed as Log(CFU) (colony forming units), Log(RV) (reduction  
317 value) and PR (percentage of reduction) are compared in the bar graphs of Figure 8 for the four  
318 bacteria, and numerical values of these results are collected in the Table S1 of the SM file. As it  
319 can be inferred from the graphs, the antimicrobial activity of both, LAE·HyA-1 and LAE·HyA-0.5,  
320 is noticeable from the earlier incubation stages so they inhibited the growth of all bacteria just  
321 after 2 h of contact. This activity was found especially important against Gram-negative bacteria  
322 so that Log(RV) values of 6.6 and 4.7 for *S. enterica*, and 3.6 and 3.9 for *E. coli* was measured  
323 for LAE·HyA-1 and LAE·HyA-0.5, respectively. This result is remarkable since Gram-negative  
324 bacteria are usually less sensible to cationic surfactants than Gram-positive bacteria due to the  
325 outer lipopolysaccharide coat that surrounds the cell wall (Vaara, 1992).

326 The antimicrobial activity of the complexes against Gram-positive bacteria was found to  
327 be lower with Log(RV) of 0.2 and 0.4 observed for *L. monocytogenes* and 1.1 and 0.4 for *S.*  
328 *aureus* for LAE·HyA-1 and LAE·HyA-0.5, respectively, after 2 h of incubation. The higher  
329 antimicrobial efficacy observed for the complex containing more LAE is quite reasonable and  
330 according to observations reported on antimicrobial films based on LAE loaded chitosan  
331 (Higueras, López-Carballo, Hernández-Muñoz, Gavara, & Rollini, 2013). However, it was  
332 interesting to see that the antimicrobial activity of the LAE·HyA-0.5 complex against *S. aureus*  
333 became higher than that of LAE·HyA-1 when long incubation times (8 and 24 h) have elapsed.  
334 This behaviour may be convincingly explained by taking into account the observations reported  
335 by Baier et al (Baier et al., 2013) on the biocide activity of HyA-based nanocapsules containing  
336 the antimicrobial agent polyhexanide. They found that *S. aureus* was particularly sensitive to the  
337 biocide agent incorporated in such systems because its release was favored by the  
338 biodegradation of HyA, a process that happened due to the action of the hyaluronidases  
339 provided by the bacteria.



340 **Figure 8.** Antimicrobial activity of LAE·HyA-1 and LAE·HyA-0.5 films over time against Gram-positive and  
 341 Gram-negative bacteria.

#### 342 4. Conclusions

343 The well recognized biocide guanidinium-based compound LAE was coupled with  
 344 hyaluronic acid to render ionic complexes with two compositions, *i.e.* LAE:HyA = 1 and 0.5.  
 345 These complexes were non-soluble in water and stable to heat up to temperatures above 200  
 346 °C. Although the genuine crystallinity of LAE was lost when it was incorporated in the complex,  
 347 a smectic liquid crystal arrangement was adopted by both LAE·HyA-1 and LAE·HyA-0.5. The

348 nanostructure of the complexes is characterized by a periodicity of about 3.8-3.9 nm  
349 corresponding to the repeating distance of an alternating array of HyA and LAE layers in which  
350 the undecyl tail of the lauroyl group of LAE is in the disordered state. These complexes  
351 dissociated upon incubation in an aqueous medium in a range of hours providing free LAE at  
352 equilibrium concentrations depending on pH and complex composition. Films prepared from  
353 these complexes displayed significant biocide activity against both Gram-positive and Gram-  
354 negative bacteria with the highest efficiency being shown by LAE-HyA-1 against *S. enterica*.

### 355 **Acknowledgements**

356 This work received financial support from MCINN (Spain) with Grant MAT2012-38044-  
357 C03 and MAT-2016-77345-CO3-03. XRD analyses realized in this research were carried out at  
358 the BL11 line of ALBA synchrotron (Cerdanyola del Vallès, Barcelona, Spain) with the  
359 invaluable support of Dr. Christina Kamma-Lorger. Thanks to Dr. Marta Fernández García from  
360 CSIC (Madrid) for her valuable comments on the methodology followed for biocide activity  
361 estimation. Authors acknowledge the LAE sample kindly gifted by Vedeqsa (LAMIRSA GROUP,  
362 Terrassa, Barcelona, Spain). Thanks also to the MICINN for the Ph.D. grant awarded to Ana  
363 Gamarra Montes.

364 **References**

- 365 Allison, D. D., & Grande-Allen, K. J. (2006). Hyaluronan: a powerful tissue engineering tool.  
366 *Tissue Eng.*, *12*, 2131–2140.
- 367 Asker, D., Weiss, J., & McClements, D. J. (2009). Analysis of the interactions of a cationic  
368 surfactant (lauric arginate) with an anionic biopolymer (pectin): Isothermal titration  
369 calorimetry, light scattering, and microelectrophoresis. *Langmuir*, *25*, 116–122.
- 370 Baier, G., Cavallaro, A., Vasilev, K., Mailänder, V., Musyanovych, A., & Landfester, K. (2013).  
371 Enzyme responsive hyaluronic acid nanocapsules containing polyhexanide and their  
372 exposure to bacteria to prevent infection. *Biomacromolecules*, *14*, 1103–1112.
- 373 Battistini, F. D., Tártara, L. I., Boiero, C., Guzmán, M. L., Luciani-Giacobbe, L. C., Palma, S.  
374 D., Allemandi D.A., Manzo, R.H., Olivera, M. E. (2017). The role of hyaluronan as a drug  
375 carrier to enhance the bioavailability of extended release ophthalmic formulations.  
376 Hyaluronan-timolol ionic complexes as a model case. *Eur. J. Pharm. Sci.*, *105*, 188–194.
- 377 Becerril, R., Manso, S., Nerin, C., & Gómez-Lus, R. (2013). Antimicrobial activity of lauroyl  
378 arginate ethyl (LAE), against selected food-borne bacteria. *Food Control*, *32*, 404–408.
- 379 Bračić, M., Hansson, P., Pérez, L., Zemljič, L. F., & Kogej, K. (2015). Interaction of sodium  
380 hyaluronate with a biocompatible cationic surfactant from lysine: a binding study. *Langmuir*,  
381 *3*, 12043–12053.
- 382 Burdick, J. A., & Prestwich, G. D. (2011). Hyaluronic acid hydrogels for biomedical applications.  
383 *Adv. Mater.*, *23*, H41–H56.
- 384 Chytil, M., Trojan, M., & Kovalenko, A. (2016). Study on mutual interactions and electronic  
385 structures of hyaluronan with lysine, 6-Aminocaproic acid and arginine. *Carbohydr. Polym.*,  
386 *142*, 8–15.
- 387 Durán, N., Marcato, P. D., De Souza, G. I. H., Alves, O. L., & Esposito, E. (2007). Antibacterial  
388 effect of silver nanoparticles produced by fungal process on textile fabrics and their effluent  
389 treatment. *J. Biomed. Nanotech.*, *3*, 203–208.

390 Engler, A. C., Wiradharma, N., Ong, Z. Y., Coady, D. J., Hedrick, J. L., & Yang, Y. Y. (2012).  
391 Emerging trends in macromolecular antimicrobials to fight multi-drug-resistant infections.  
392 *Nano Today*, 7, 201–222.

393 Gamarra-Montes, A., Missagia, B., Morató, J., & Muñoz-Guerra, S. (2017). Antibacterial films  
394 made of ionic complexes of Poly( $\gamma$ -glutamic acid) and ethyl lauroyl arginate. *Polymers*, 10,  
395 1–15.

396 Gilli, R., Kacurakova, M., Mathlouthi, M., Navarini, L., Paoletti, S. (1994). FTIR studies of  
397 sodium hyaluronate and its oligomers in the amorphous solid-phase and in aqueous-  
398 solution. *Carbohydr. Res.*, 263, 315-326

399 Hanski, S., Houbenov, N., Ruokolainen, J., Chondronicola, D., Latrou, H., Hadjichristidis, N., &  
400 Ikkala, O. (2006). Hierarchical ionic self-assembly of rod-comb block copolypeptide-  
401 surfactant Complexes. *Biomacromolecules*, 7, 3379–3384.

402 Higuera, L., López-Carballo, G., Hernández-Muñoz, P., Gavara, R., & Rollini, M. (2013).  
403 Development of a novel antimicrobial film based on chitosan with LAE (ethyl-*N*-  
404 dodecanoyl-*L*-arginate) and its application to fresh chicken. *Int. J. Food Microbiol.* 165,  
405 339–345.

406 Kemp, M. M., Kumar, A., Clement, D., Ajayan, P., Mousa, S., & Linhardt, R. J. (2009).  
407 Hyaluronan- and heparin-reduced silver nanoparticles with antimicrobial properties.  
408 *Nanomedicine*, 4, 421–429.

409 Lequeux, I., Ducasse, E., Jouenne, T., & Thebault, P. (2014). Addition of antimicrobial  
410 properties to hyaluronic acid by grafting of antimicrobial peptide. *Eur. Polym. J.*, 51, 182–  
411 190.

412 Liu, L., Liu, Y., Li, J., Du, G., & Chen, J. (2011). Microbial production of hyaluronic acid: current  
413 state, challenges, and perspectives. *Microbiol. Cell Fact.*, 10, 99–108.

414 Loeffler, M., McClements, D. J., Mclandsborough, L., Terjung, N., Chang, Y., & Weiss, J. (2014).  
415 Electrostatic interactions of cationic lauric arginate with anionic polysaccharides affect

416 antimicrobial activity against spoilage yeasts. *J. Appl. Microbiol.*, 117, 28–39.

417 Macknight, W. J., Ponomarenko, E. A., & Tirrel, D. A. (1998a). Self-assembled polyelectrolyte-  
418 surfactant complexes in nonaqueous solvents and in the solid state. *Acc. Chem. Res.*, 31,  
419 781–788.

420 Macknight, W. J., Ponomarenko, E. A., & Tirrel, D. A. (1998b). Stoichiometric complexes of  
421 synthetic polypeptides and oppositely charged surfactants in organic solvents and in the  
422 solid state. *Macromolecules*, 29, 8751-8758.

423 Necas, J., Bartosikova, L., Brauner, P., & Kolar, J. (2008). Hyaluronic acid (hyaluronan): a  
424 review. *Vet. Med.*, 53, 397–411.

425 Otero, V., Becerril, R., Santos, J. A., Rodríguez-Calleja, J. M., Nerín, C., & García-López, M. L.  
426 (2014). Evaluation of two antimicrobial packaging films against *Escherichia coli* O157: H7  
427 strains in vitro and during storage of a Spanish ripened sheep cheese (Zamorano). *Food*  
428 *Control*, 42, 296–302.

429 Pérez-Camero, G., García-Álvarez, M., Martínez de Ilarduya, A., Fernández, C., Campos, L., &  
430 Muñoz-Guerra, S. (2004). Comb-like complexes of bacterial poly( $\gamma$ ,D-glutamic acid) and  
431 cationic surfactants. *Biomacromolecules*, 5, 144–152.

432 Ponomarenko, E.A., Waddon, A.J., Tirrell, D.A. & MacKnight, W.J. (1996). Structure and  
433 properties of stoichiometric complexes formed by sodium poly( $\alpha$ ,L-glutamate) and  
434 oppositely charged surfactants. *Langmuir*, 12, 2169–2172.

435 Rodriguez, E., Seguer, J., Rocabayera, X., & Manresa, A. (2004). Cellular effects of  
436 monohydrochloride of *L*-arginine, *N*-alpha-lauroyl ethylester (LAE) on exposure to  
437 *Salmonella typhimurium* and *Staphylococcus aureus*. *J. Appl. Microbiol.*, 96, 903–912.

438 Santos, M. R. E., Fonseca, A. C., Mendonça, P. V., Branco, R., Serra, A. C., Morais, P. V., &  
439 Coelho, J. F. J. (2016). Recent developments in antimicrobial polymers: a review.  
440 *Materials*, 9, 599-632.

- 441 Schanté, C. E., Zuber, G., Herlin, C., & Vandamme, T. F. (2011). Chemical modifications of  
442 hyaluronic acid for the synthesis of derivatives for a broad range of biomedical applications.  
443 *Carbohydr. Polym.*, 85, 469-489.
- 444 Stern, R., Kogan, G., Jedrzejas, M. J., & Šoltés, L. (2007). The many ways to cleave  
445 hyaluronan. *Biotechnol. Adv.*, 25, 537–557.
- 446 Tolentino, A., Alla, A., Martínez de Ilarduya, A., & Muñoz-Guerra, S. (2011). Comb-like ionic  
447 complexes of pectinic and alginic acids with alkyltrimethylammonium surfactants.  
448 *Carbohydr. Polym.*, 86, 484–490.
- 449 Tolentino, A., Alla, A., Martínez de Ilarduya, A., & Muñoz-Guerra, S. (2013). Comb-like ionic  
450 complexes of hyaluronic acid with alkyltrimethylammonium surfactants. *Carbohydr. Polym.*,  
451 92, 691–696.
- 452 Vaara, M. (1992). Agents that increase the permeability of the outer membrane. *Microbiol. Rev.*,  
453 56, 395–411.